An Infralimbic Cortex Neuronal Ensemble Encoded During Learning Attenuates Fear Generalization Expression

Rajani Subramanian[1], Avery Bauman[1], Olivia Carpenter[1], Chris Cho[1], Gabrielle Coste[1], Ahona Dam[1], Kasey Drake[1], Sara Ehnstrom[1], Naomi Fitzgerald[1], Abigail Jenkins[1], Hannah Koolpe[1], Runqi Liu[1], Tamar Paserman[1], David Petersen[1], Diego Scala Chavez[1], Stefano Rozental[1], Hannah Thompson[1], Tyler Tsukuda[1], Sasha Zweig[1], Megan Gall[2], Bojana Zupan[1], Hadley Bergstrom[1]

[1] Department of Psychological Science, Program in Neuroscience and Behavior, Vassar College, Poughkeepsie NY 12603 USA

[2] Department of Biology, Program in Neuroscience and Behavior, Vassar College, Poughkeepsie NY 12603 USA

Key words: Engram, Risk assessment, Contextual fear, Predator imminence continuum theory, Extinction, Individual differences

Correspondence: Hadley Bergstrom, PhD, Department of Psychological Science, Program in Neuroscience & Behavior, Vassar College, Poughkeepsie, NY 12604 USA, email: habergstrom@vassar.edu

ABSTRACT

Generalization allows for experience to flexibly guide behavior when conditions change. A basic physical unit of memory storage and expression in the brain are sparse, distributed groups of neurons known as ensembles (i.e., the engram). The infralimbic (IL) subregion of the ventral medial prefrontal cortex plays a key role in modulating conditioned defensive responses. How IL neuronal ensembles established during learning contribute to generalized responses is unknown. In this set of experiments, generalization was tested in male and female mice by presenting a novel, ambiguous, tone generalization stimulus following Pavlovian defensive (fear) conditioning. The first experiment was designed to test a role for IL in generalization using chemogenetic manipulations. Results show IL bidirectionally regulates defensive behavior. IL silencing promotes a switch in defensive state from vigilant scanning to generalized freezing, while IL stimulation reduces freezing in favor of scanning. Leveraging activity-dependent tagging technology (ArcCreER^{T2} x eYFP system), a neuronal ensemble, preferentially located in IL superficial layer 2/3, was associated with the generalization stimulus. Remarkably, in the identical discrete location, fewer reactivated neurons were associated with the generalization stimulus at the remote timepoint (30 days) following learning. When an IL neuronal ensemble established during learning was selectively chemogenetically silenced, generalization increased. Conversely, IL neuronal ensemble stimulation reduced generalization. Overall, these data identify a crucial role for IL in suppressing generalized responses. Further, we uncover an IL neuronal ensemble, formed during learning, functions to later attenuate the expression of generalization in the presence of ambiguous threat stimuli.

INTRODUCTION

When confronted with a clear and present threat, organisms must respond appropriately for defense. Sometimes threats are unclear, or ambiguous, which might call for a more flexible, or generalized response, based on past experience (Richards & Frankland, 2017). In the field of psychology, generalization refers to the transfer of conditioned responses to stimuli that are similar, but not identical, to the original conditioned stimulus (Guttman & Kalish, 1956). Generalization was first described over a century ago (Pavlov, 1927; Watson & Rayner, 1920), is highly conserved across species (Dymond et al., 2015; Orr & Lukowiak, 2008), and has even been proposed as one of the only universal laws in the field of psychology (Shepard, 1987). While generalization is evolutionarily adaptive, overgeneralization of defensive behavior is maladaptive, and relevant to understanding posttraumatic stress disorder (PTSD) and anxiety-related disorders (Cooper et al., 2022; Dunsmoor & Paz, 2015). The fundamental nature of stimulus generalization, in both the study of basic memory processes and clinical disorders, makes the investigation of generalization a central topic in the field of neuroscience (Sangha et al., 2020).

The ventral medial prefrontal cortex (vmPFC), and infralimbic (IL) subregion (cingulate cortex Area 25), is an identified hub in the defensive conditioning circuit (Sotres-Bayon et al., 2006). Functionally, a role for IL in extinction processes is canonical (Giustino & Maren, 2015). A growing number of studies have also indicated IL functionality in generalization (Bayer & Bertoglio, 2020; Corches et al., 2019; Day et al., 2020; Kreutzmann et al., 2020; Kreutzmann & Fendt, 2020; Ng et al., 2023; Sangha et al., 2014; Scarlata et al., 2019). The consensus from these studies is that IL functionality mediates memory specificity by attenuating generalization.

The term neural ensemble or “engram” refers to a sparse, distributed, group of neurons that forms a physical substrate of memory in the brain (Josselyn et al., 2015). An approach for studying neuronal ensembles is the use of molecular genetic tools for the selective expression

(or “tagging”) of fluorescent molecules, or optogenetic and chemogenetic actuators, during learning for later visualization and manipulation during memory retrieval (DeNardo & Luo, 2017). One such system is the ArcCreER^{T2} x eYFP mouse line. In this system, activity-dependent Arc gene transcription, a key component in learning and memory-induced synaptic plasticity, leads to the expression of a CreER^{T2} fusion protein which, upon activation with a synthetic estrogen receptor (ER) agonist (i.e., 4-OHT), leads to Cre-induced recombination and expression of a fluorescent molecular tag (Denny et al., 2014).

Generalization has long been proposed to be established during learning (Hull, 1943), although this hypothesis has not been tested. Here, we designed a set of experiments to determine whether an IL neuronal ensemble encoding an inhibitory process is established during Pavlovian defensive conditioning. We hypothesize that after learning, this ensemble contributes to memory specificity by reducing conditioned responses to generalization stimuli. The ArcCreER^{T2} x eYFP transgenic mouse system is particularly advantageous for addressing this question because neurons activated during learning can be later manipulated under conditions that promote generalization.

To first establish a role for IL activity in cued fear memory generalization we used a Designer Receptors Exclusively Activated by Designer Drugs (DREADD) system and CaMKII promotor to bidirectionally control IL excitability during the expression of generalization. In the second set of experiments, we took advantage of the ArcCreER^{T2} x eYFP system to visualize and measure IL neuronal ensembles associated with generalization at recent and remote timepoints following learning. In the final set of experiments, a double-floxed inverse open reading frame (DIO)-DREADD system in combination with ArcCreER^{T2} x eYFP transgenic mice was used to transfect DREADDs constructs in Arc-expressing neurons during learning for later synthetic chemical manipulation during memory retrieval.

MATERIALS and METHODS

Animals

Adult male and female ArcCreER^{T2} x eYFP mice were used in all experiments. B6.Cg-Tg(Arc-cre/ERT2)MRhn/CdnyJ (ArcCreER^{T2}) mice were crossed with B6.129X1-Gt(ROSA)26Sor$^{tm1(EYFP)Cos}$/J (eYFP) mice (Jackson laboratory strain #022357 and strain #006148, respectively) to produce double transgenic mice (hereafter referred to ArcCreER^{T2} x eYFP mice). ArcCreER^{T2} x eYFP mice were bred on-site over multiple generations and were used in all experiments. At the memory retrieval stage of all experiments, adults ranged from 71 – 150 days old (mean = 112.5 ± S.D. 27.8) (female weight = 16.4 – 32.9 g, median weight = 22.1; male weight = 21.9 – 42.8 g, median weight = 30.4). Same sex mice were group-housed (2-5/cage) in individual vented standard cages, except when singly housed after surgery. There were three types of enrichment in each cage, including a wood gnawing block, nestlet, and EnviroPAK. The vivarium temperature (23 - 25 ^{o}C), humidity (35 - 37%), and 12 hr light/dark cycle (lights on 0600) were controlled throughout. Food and water were available *ad libitum* and cages were changed 1 x/week. Mice were randomly assigned to experimental groups based on litter before the start of each experiment. All experimental procedures were conducted in accordance with the National Institutes of Health guidelines on the Care and Use of Animals in Research and approved by the Vassar College Institutional Use and Animal Care Committee (IACUC). Disclosure of animal housing, husbandry, and experimental procedures follow principles for transparent reporting and reproducibility in behavioral neuroscience (Prager et al., 2011, 2018).

Genotyping protocol

Tissue biopsy was performed by tail snip under brief isoflurane anesthesia. DNA was extracted using DirectPCR Lysis Reagent (Viagen Biotech, Los Angelas CA) following

manufacturer protocol. Amplification of Cre and R26R was performed using the following primer sets: *Cre*: 5′-GCC TGC ATT ACC GGT CGA TGC AAC G-3′; 5′-AAA TCC ATC GCT CGA CCA GTT TAG TTA CCC-3′. *R26R* (for *EYFP* mice) 5′-GGA GCG GGA GAA ATG GAT ATG-3′; 5′-AAA GTC GCT CTG AGT TGT TAT-3′; 5′-AAG ACC GCG AAG AGT TTG TC-3′, following recommended cycling protocols from Jackson Labs and Denny et al., 2014.

General behavioral experimental procedures

All experiments were performed during the light cycle. A background strain of the ArcCreER^{T2} x eYFP mouse is the C57BL/6J (B6) mouse, which is an age-related hearing decline model (Ison et al., 2007). Hearing decline in B6 mice in complex, but low frequency hearing, which is relevant to this study, has consistently been shown to decline with age. To address this, no mice over 150 days old were tested. We also evaluated peripheral auditory brainstem responses to relevant frequencies (see below). All mice were habituated to a holding room 30-45 m prior to conditioning and testing. To reduce contextual (background) freezing, the training context (hereafter referred to as “Context A”) was disguised from the testing context (hereafter referred to as “Context B”) using several manipulations. Context A was an unmodified fear conditioning chamber (Coulbourn Instruments, Holliston, MA) and a 70% EtOH solution was used to clean the chambers between mice. For context B, (1) mice were transferred from the vivarium to the holding room using distinctive cages, carts, and covering, (2) the ambient lighting and background noise of the holding and testing room were changed using different illuminance and a fan for background noise, (3) a white plexiglass floorboard sprinkled with clean bedding was used to cover the shock bars, (4) the testing chamber walls were disguised with black- and white-striping, (5) the chambers were cleaned with a 1% acetic acid solution between mice (Bergstrom, 2020). Each day, prior to training and testing, the decibel level (dB) for the auditory tone frequency was measured in each chamber using a sound level meter (R8050, REED Instruments, Wilmington, NC) and calibrated to 70-75 dB. All conditioning was

conducted in commercial chambers (20 x 30 x 18 cm) in sound-dampening cabinets (58 x 61 x 45 cm) (Colbourn instruments, Holliston, MA). FreezeFrame 4 software was used for controlling and delivering the tone and foot shock stimuli (ActiMetrics, Wilmette, IL). All acoustic stimuli were delivered by a speaker mounted on the upper center of one wall and foot shock stimuli were delivered via a stainless-steel rod floor (0.8 cm distance between rods, 1.0 cm rod diameter).

Fear conditioning

Mice were placed in the fear conditioning chamber (Context A) 180 s prior to 3 pairings of an auditory tone CS (20 s, 5-kHz, 70-75 dB) that co-terminated with an electric foot shock US (0.5 s, 0.5 mA). The CS/US pairings were separated by variable inter-trial intervals (ITI) (20 and 80 s). Mice were removed from the chamber 60 s after the final CS/US pairing. The total conditioning time was 400 s.

Context B pre-exposure

To reduce “background” generalized contextual freezing (Jacobs et al., 2010), mice were placed into Context B for 15 m and left to explore on the day prior to the cued generalization test (Bergstrom, 2020).

Generalization test

Either 6 days (recent group) or 30 days (remote group) following training (1 day following Context B pre-exposure) mice were placed in Context B prior to 3 presentations either the CS (5-kHz, 70-75 dB, 20 s) or a novel tone generalization stimulus (GS; 3-kHz, 70-75 dB, 20 s). A 3-kHz tone GS was used because in previous experiments, following conditioning with a 5-kHz CS, it produced the greatest degree of generalization over time in comparison with alternate tone frequencies (Pollack et al., 2018). The novel 3-kHz tone GS was dubbed the “ambiguous” stimulus throughout. Mice were removed from the chamber 60 s after the final stimulus

188 presentation and returned to the colony room (400 s total test time; ITIs 80 and 20 s). Mice in
189 the “no tone” control group were allowed to explore context B for 400 s.

190 Genetic labeling procedures

191 To reduce non-specific genetic labeling, mice were dark-housed the night before and
192 three days following the 4-OHT injection. These methods have been previously validated
193 (Cazzulino et al., 2016; Denny et al., 2014). For dark housing procedures, mice were placed in a
194 separate housing room with lights off, limited noise, and no handling. ArcCreER^{T2} X eYFP mice
195 were intraperitoneally (i.p.) injected with 4-OHT exactly 5 h prior to fear conditioning. This
196 timeframe has been previously validated (McGowan et al., 2024).

197 Drugs

198 4-Hydroxytamoxifen (4-OHT)

199 Cre-mediated recombination in ArcCreER^{T2} x eYFP mice was induced using 4-OHT
200 (HelloBio, Princeton NJ; SKU: HB6040). 4-OHT was made fresh prior to each injection (i.p.). 4-
201 OHT was dissolved by water bath sonication in a 10% EtOH/90% corn oil solution at 10 mg/mL.
202 The final dose was 55 mg/kg.

203 DREADD actuators

204 Clozapine N-oxide (CNO)

205 For the CaMKII-DREADD experiments, CNO was used as the chemical actuator (Hello
206 Bio, Princeton NJ SKU: HB6149). It was made fresh prior to i.p. injection, dissolved in 0.9%
207 saline (1 mg/mL), and injected i.p. (5.0 mg/kg) exactly 45 m prior to the memory test.

208 Deschloroclozapine dihydrochloride (DCZ)

For DIO-DREADD experiments, DCZ was used as the chemical actuator (Nagai et al., 2020) (Hello Bio, Princeton, NJ, SKU: HB9126). It was made fresh immediately prior to i.p. injection, dissolved in 0.9% saline (1 mg/mL), and injected i.p. at 100 µg/kg exactly 15 m prior to the memory test.

Immunohistochemistry

Tissue collection

Exactly 90 m following the fear memory retrieval test, all mice were injected with a ketamine/xylazine cocktail (100:10 mg/mL) and transcardially perfused with ice-cold 1X PBS (7.2 - 7.4 pH), followed by ice-cold 4% paraformaldehyde (PFA) in 1X PBS (7.2 - 7.4 pH). The time point for perfusion following the retrieval test was based on several previous reports (Maddox and Schafe, 2011; Ploski et al., 2008). Brains were extracted and placed into 4% PFA overnight at 4°C then transferred to 1X PBS and kept at 4°C until sectioning. Coronal brains sections (40 μm thick) were cut through the mPFC using a vibratome (VT1200, Leica Biosystems Inc., Buffalo Grove, IL). Every other section (to avoid double-counting) was collected in a well plate containing 1X PBS (7.4 pH) for free-floating immunohistochemistry. Sections were rinsed first in 1X PBS (3 x 10 m), blocked in a 1X PBS/1% bovine serum albumin (BSA)/0.2%Triton-X solution for 1 hour, and incubated in antigen specific antibodies (see below). All incubations were performed on orbital shakers.

Arc and eYFP primaries

After blocking, sections were incubated overnight in Anti-Arc rabbit polyclonal antibody (1:5000) (Cat No. 156003, Synaptic Systems, Goettingen, Germany) and Anti-GFP chicken polyclonal antibody (1:10000) (Cat No.13970, Abcam, Waltham, MA) at 4°C. The next day, sections were washed in 1X PBS (3 x 10 m) before a 1 h incubation in Donkey anti-rabbit IgG (1:1000) (#A32754, Invitrogen) and Goat anti-chicken IgG (1:500) (Cat No. A32931, Invitrogen) at room temperature.

c-Fos

To test the efficacy of CNO to activate the DREADDs system (either hM4Di or hM3Dq), a subset of mice, having completed all behavioral testing, received i.p. injections of CNO at 5.0 mg/kg dosage and were placed into the Context B recall test after 45 m (peak expression time) (Campbell & Marchant, 2018). Exactly 135 m after CNO injection and 90 m after recall (peak c-Fos expression) (Barros et al., 2015), mice were sacrificed for IHC. All procedures for IHC were identical to those described above except that sections were then incubated for 24 hours with anti-c-Fos rabbit polyclonal antibody (1:500) (Cat No. RPCA-c-Fos, RRID: AB_2572236, EnCor Biotechnology Inc., Gainesville, FL USA) at room temperature. For the secondary antibody, subjects in either the pAAV-CaMKIIa-hM4Di-mCherry or pAAV-CaMKIIa-hM3Dq-mCherry groups were incubated with Alexa Fluor 488 goat anti-rabbit IgG (H+L) (Lot #: 1981125, REF: A11008, Invitrogen, Carlsbad, CA USA) and pAAV-CaMKIIa-EGFP subjects were incubated with Alexa Fluor 594 donkey anti-rabbit IgG (H+L) (Lot #: WD319534, REF: A32754, Invitrogen, Carlsbad, CA USA) for one hour at room temperature.

DIO-DREADD Arc

To test the efficacy of DCZ to activate the DIO-DREADDs system (either hM4Di or hM3Dq) and modify Arc expression in preferentially transfected cell populations, mice were injected with DCZ 105 m prior to fear conditioning and processing for Arc IHC. The timeline for DCZ injection were based on high DCZ brain level concentrations at 15 m (Nagai et al., 2020) and peak Arc expression at 90 m following fear conditioning (Maddox and Schafe, 2011; Ploski et al., 2008). The experimental procedures for IHC were identical to those describe above for Arc IHC except the secondary antibody for Arc was Donkey anti-rabbit IgG (Alexa Fluor 647) (1:1000) (Lot #: YF374181, REF: A32795, Invitrogen, Carlsbad, CA USA).

Tissue mounting

Following all incubations, sections were rinsed a final time in 1X PBS (3x10 m) then mounted onto gel-coated slides in 0.05M PB. Sections were cover slipped (#1 or #1.5 thickness)

using Fluoromount-G mounting medium with DAPI (#00-4959-52, Invitrogen) and sealed with nail polish. Slides were stored at 4°C in darkness until imaging.

Image acquisition and analysis

Images were acquired using a Leica TCS SP5 II laser scanning confocal with the Leica Microsystems LAS AF software (Version: 2.6.0.7266). The objective used was a Leica HCX PL APO CS 20X/.70 Dry. 3D images were acquired by taking a z stack of 20-30 slices with 1.14 µm spacing and pixel dimensions 760 x 760 nm. Images for the DIO-DREADD experiment were captured using the Leica Stellaris 8 FALCON laser scanning confocal platform.

The experimenter was blind to experimental conditions throughout all neuronal ensemble quantification procedures. Cell counts were acquired by sampling across 6 IL regions/subject. IL sampling regions for data collection were chosen based on the quality of the staining and visibility of anatomical landmarks for localization of the counting frame (see below), Labeled cells were quantified using FIJI. Background subtraction was applied across all channels. For c-Fos microscopy, images were captured under fluorescent microscope (Nikon Eclipse 50*i*, Nikon Instruments, Amsterdam, NL). c-Fos$^+$ cells were counted manually (FIJI-ImageJ open source) in the mPFC using a counting frame (250 x 250 μm) with AAV$^+$ and adjacent AAV$^-$ expression area and six locations/subject (mCherry$^+$ n = 6, eYFP$^+$ n = 6).

To locate IL and PL for placement of the counting frame, the lateral ventricle (LV) was used as an anatomical landmark, as it is readily identifiable and located in a consistent position ventral to the IL, and aligned with DP, for a majority of the longitudinal axis. Midline and the corpus collosum were also used as stable anatomical landmarks to identify the location of the IL and PL. For the IL, the counting frame (250 x 250 μm) was positioned approximately 600 μm dorsal from the LV. For the PL, the counting frame was positioned 1250 μm dorsal from LV. For layer measurements, the counting frame was centered 300 μm from midline for L2/3 (shallow layers) and 500 μm (deep) from midline for L5/6. Cells in the IL were counted between rostrocaudal levels of bregma 1.93 and 1.53 (Paxinos & Franklin, 2019). DAPI cells were

counted using the 3D object counter in FIJI. Fluor 488+, Fluor 594+, and co-labeled cells were counted manually within the counting frame. Colocalized $eYFP^+$:Arc^+ neurons were first analyzed as a percentage of the number of $DAPI^+$ neurons. Chance rate neuronal co-localization was calculated as: ($eYFP^+$/$DAPI^+$) * (Arc^+/$DAPI^+$) * 100.

DREADDS

Viral Constructs

All viral constructs were purchased from Addgene (Watertown MA). In the first set of experiments, pAAV-CaMKIIa-hM4Di-mCherry (AAV5), pAAV-CaMKIIa-hM3Dq-mCherry (AAV8), or a fluorophore-only control AAV (pAAV-CaMKIIa-EGFP; AAV5) was used. In the DIO-DREADD experiments, pAAV-hSyn-DIO-hM4D(Gi)-mCherry (AAV8), pAAV-hSyn-DIO-hM3D(Gq)-mCherry (AAV8), or fluorophore control AAV (pAAV-hSyn-DIO- mCherry (AAV8) was used. All viral vectors were aliquoted and stored at -80 C until use.

Surgery

Prior to surgery, mice received an injection of carprofen (s.c., 5.0 mg/kg) and an intradermal injection of bupivacaine (0.05 mL) at the craniotomy site. Inhaled isoflurane levels were maintained between 1.25% - 2.5% throughout. Mice were bilaterally microinjected (100-150 nL/hemisphere) with either the hM4Di, hM3Dq, or fluorophore-control AAV targeting the IL (stereotaxic coordinates: AP: +1.8, ML: +0.3/-0.3, DV: -2.8). Microinjections were conducted using a 2.5 µL glass syringe and 32-gauge needle (Hamilton, Reno NV). Following surgery, a dietary supplement (DietGel Recovery Purified) and carprofen (s.c., 5.0 mg/kg) was provided as needed. Subjects were singly housed for two weeks and group-housed, if possible, prior to behavioral testing. Fear conditioning occurred no less than two weeks following stereotaxic surgery. All fear conditioning and generalization experimental parameters were identical to those described above.

On generalization test day, mice were injected (i.p.) with CNO 45 m prior to testing. The following day, mice were injected (i.p.) with saline (same volume as CNO) using procedures

identical to those described above for CNO and were run through the generalization test protocol again.

DIO-DREADD methods

To manipulate neuronal ensemble reactivation, a Cre-dependent viral construct expressing either an excitatory DREADD (pAAV-hSyn-DIO-hM3D(Gq)-mCherry), inhibitory DREADD (pAAV-hSyn-DIO-hM4D(Gi)-mCherry) or a fluorophore control (pAAV-hSyn-DIO-mCherry) was injected into the IL of ArcCreER^{T2} x eYFP mice. After at least 2 weeks, on the fear conditioning day, all mice were injected with 4-OHT to drive Cre-recombination and DIO-DREADD expression in neurons with high levels of Arc. This permits specific expression of DREADDs constructs in activated cellular populations for later reactivation or silencing using the actuator DCZ.

Either 6 days (recent group) or 30 days (remote group) following training (1 day following Context B pre-exposure), mice were injected with DCZ 15 m prior to the generalization test. 90 m following testing, all mice were sacrifice for Arc IHC (see above).

Behavioral analysis

Freezing

An overhead camera recorded digital video of the fear conditioning chamber. Freezing behavior was automatically quantified using FreezeFrame 4.0 (ActiMetrics, Wilmette IL). Freezing was defined as the lack of movement except for respiration for >1 s (FreezeFrame threshold = 5). Percentage freezing data was calculated by scoring freezing during the CS or GS presentations (20 s), pre-CS/GS period (habituation), and inter-trial intervals (ITIs).

Scanning

Scanning was operationally defined as a side-to-side head and front paw movement while the tail base remained motionless. Scanning behavior was recorded immediately upon initiation and halted when the mouse, 1) froze >1 s or, 2) initiated full movement. Movement was

337 defined as a larger category of behaviors, including four-paw locomotion, grooming, rearing, and
338 small, jerk-like body and head movements, not identified as freezing or scanning.

339 Pose estimation for each video was created using DeepLabCut version 2.3.10. Each
340 video was 400 s long and recorded at 8 frames/s (fps), resulting in 3,000 frames/video. Fifty
341 randomly sampled frames from each video were manually labeled, with the nose and tail base
342 serving as the labeling points.

343 To train the ResNet-50 network, 95% of the labeled frames were used, while the
344 remaining 5% were reserved for testing the neural network's performance. Each video
345 underwent over 10,000 training iterations, yielding a training error of 8.02 pixels and a test error
346 of 8.61 pixels. By applying a p-cutoff of 0.4, the training error was reduced to 7.22 pixels, though
347 the test error remained unchanged.

348 A separate Python script was developed to extract freezing and scanning behaviors from
349 DeepLabCut (DLC)output, which included pose estimations of nose and tail base. This script
350 averaged the coordinates over 8 frames to determine the coordinates/s. It then calculated the
351 velocity (pixels/s) of nose and tail base/s. The script identified freezing and scanning behaviors
352 using criteria established through extensive comparisons between test results, hand-scored,
353 and Freezeframe 4.0 results (ActiMetrics, Wilmette IL) (Figure S1). In DLC, freezing behavior
354 was defined as the velocity of both the nose and tail base being < 6 pixels/s with immobility
355 lasting >1 s. Scanning behavior was defined as the nose velocity >10 pixels/s, and tail base
356 velocity <10 pixels/s.

357 Auditory Brain Stem Responses

358 To determine auditory thresholds, a set of 5-ms tonebursts (1-ms Blackman-Harris
359 gating) was generated in SigGenRZ (v 5.6.0). We generated stimuli at nine frequencies (1, 2,
360 2.5, 3, 3.15, 4, 8, 10, and 12.5 kHz) that spanned the frequency range of stimuli used in the

generalization experiments. We also generated broadband clicks that were periodically presented to the animals to track physiological stability across the course of the experiment. Peak-to-peak equivalent stimuli levels were determined with a Larson Davis LXT sound level meter and a long-duration 1 kHz tone. We calibrated the frequency response of the speaker with long-duration tones in 1/3 octave bands with a Larson Davis LXT sound level meter (fast, z-weighting). Frequency-specific output levels were adjusted using the gain function in SigGenRZ until a flat frequency response was achieved (± 1 dB).

All tests were performed in a 1.8 m x 1.9 m x 2 m IAC acoustics (Naperville, IL) audiology booth lined with pyramidal acoustic foam to provide sound deadening. We used electrode placement and stimulus presentation rates previously used. Each subject was anesthetized with an injection (i.p.) of ketamine (90 mg/kg) and xylazine (10 mg/kg) solution. The subject was placed on a heating pad covered with surgical towels. When the animal no longer responded to a toe-pinch, we cleaned the skin with 70% isopropyl alcohol and three 27-gauge 12 mm subdermal needles (Rochester Electro-Medical Inc.; Lutz, FL) were inserted: one non-inverting (active) electrode at the vertex of the head, one inverting (reference) electrode directly below the auditory meatus of the right ear, and one grounding electrode directly below the auditory meatus of the left ear. The electrode leads were connected to a Tucker Davis Technologies (TDT; Alachua, FL) RA4LI head stage and RA4PA preamp, which then fed into a TDT RZ6 processor via a fiber optic cable. After placing the electrodes, the impedance of the electrode was checked and repositioned if necessary to maintain an impedance at or below 5 kΩ. During the experiment layers of surgical towel were periodically added or removed to maintain body temperature.

Stimulus presentation and evoked potential recordings were coordinated by BioSigRZ (v 5.6.0), a POE5 signal processing card, and the RZ6 processor. Stimuli were presented at a rate of 31.1 stimuli s-1 from an Orb Mod2 satellite speaker (Orb Audio, U.S.A.; frequency response:

386 0.12 – 15 kHz) positioned 10 cm from the right ear of the subject. Different stimulus amplitude
387 intervals were used depending on known thresholds for each frequency to assess thresholds
388 more rapidly. Typically, larger steps (10 or 20 dB) were used farther away from the threshold
389 and smaller steps (5 dB) were used near the threshold. The exact set of stimuli amplitudes
390 varied by frequency. Two sets of 400 stimuli were played in alternating phases for each
391 combination of stimulus frequency and amplitude. Between each set of frequencies, we also
392 assessed the response to a pair of clicks presented at 80 dB to monitor the physiological
393 stability of the subject. Evoked responses were notch-filtered at 60 Hz and band-pass filtered
394 between 0.03 – 3 kHz.

395 Auditory thresholds at each frequency were determined using visual detection, where
396 two trained observers independently identified the lowest stimulus amplitude evoking a
397 response. Thresholds were estimated as the sound pressure level halfway between that of the
398 last detectable response and the next quietest stimulus. Since stimulus intensities in threshold
399 regions differed by 5 dB, ABR thresholds were defined as the intensity 2.5 dB below the lowest
400 stimuli amplitude at which a response could be visually detected.

401 Statistics

402 For all behavioral data, a mixed ANOVA was used to compare the conditioned freezing
403 response across CS/GS and ITI presentations (within-subject variable) across groups. Male and
404 female mice were included in all experiments in a full factorial experimental design. All data
405 were first checked for normality using Mauchley's test for sphericity. Violation of the assumption
406 of sphericity was addressed by adjusting the degrees of freedom using the Greenhouse-Geisser
407 correction. For some analyses, a generalization index was calculated and compared across
408 groups. The generalization index was calculated by dividing the mean of the CS by the sum of
409 CS and GS [CS / (CS + GS)]. Although the generalization index range is 1 to 0, a value of 1

410 indicates no generalization (pure discrimination) and a value of 0.5 indicates complete
411 generalization.

412 For the ArcCreER^{T2} x eYFP tagging experiments, a multivariate analysis of variance
413 (MANOVA) was used to test the statistical relationship among eYFP$^+$, Arc$^+$, or eYFP$^+$:Arc$^+$ co-
414 labeled cells in L2/3 and L5/6 of the PL and IL at different kHz frequencies (0-kHz control, 3-
415 kHz, 5-kHz) and time points (Recent or Remote) following learning. Statistics were run on the
416 number of eYFP$^+$ / DAPI$^+$, Arc$^+$ / DAPI$^+$, eYFP$^+$:Arc$^+$ / DAPI$^+$ neurons compared with the chance
417 rate of co-activation (eYFP$^+$ / DAPI$^+$) * (Arc$^+$ / DAPI$^+$) * 100), and the number of eYFP$^+$: Arc$^+$ /
418 DAPI$^+$ neurons minus chance rate (Reijmers et al., 2007; Tayler et al., 2013). Box's M test was
419 used to test the equality of variance-covariance matrices. Violation of the homogeneity
420 assumption was followed up by a rank order transformation. A significant value for the
421 conservative Pillai's Trace test statistic was only followed up by Bonferroni-corrected univariate
422 ANOVAs. Follow-up ANOVAs were checked for the assumption of equality of covariance
423 matrices using Levine's test. The Welsch test was used in the case of a significant Levine's test.
424 A significant ANOVA was followed up with a Scheffe post hoc test. Prior to analysis, outliers
425 were determined by calculating the interquartile range for each group. Any values > 1.5 steps
426 beyond the interquartile range were considered outliers and removed from the analysis. These
427 are reported in the results. Cohen's *d* values are reported for all univariate ANOVA tests. In all
428 analyses, sex was included as interacting variables in a full factorial design. For all statistics,
429 significance was set at $p<.05$. All data are represented as the mean ± the standard error of the
430 mean (SEM). All group sizes can also be found in the figure captions. Group sizes were based
431 on previous studies (Pollack et al., 2018; Scarlata et al., 2019). Statistics were run on SPSS
432 (IBM, Armonk, NY v. 26).

433

434

RESULTS

Experiment 1: Bidirectional IL chemogenetic control during the expression of cue fear memory generalization.

DREADDs system efficacy

Microinjections of the stimulatory DREADD (hM3Dq), inhibitory DREADD (hM4Di), or fluorophore control were administered into the IL at least 2 weeks prior to behavioral testing or c-Fos analysis (Figure 1A). To assess the efficacy of the DREADDs system, we analyzed mPFC c-Fos$^+$ cell density after both hM3Dq and hM4Di CNO-induced stimulation. Results showed robust CNO-induced effects across DREADDs constructs (F[2, 13]=38.8; p<.001), with increased (p<.001), and decreased (p<.01), c-Fos$^+$ cell density relative to the fluorophore control, respectively (Figure 1B and C). All injections were stereotaxically biased towards vmPFC coordinates to avoid transfection in the dorsal medial prefrontal cortex (dmPFC). After exclusion of mice with dmPFC transfection, histological analysis mapping the extent of viral transfection across individually aligned brains in stereotaxic group space confirmed AAV transfection predominantly located to IL, with some expression in dorsal peduncular cortex (PD) (Figure 1D).

Fear generalization test during IL manipulation

CNO was injected prior to a cued fear memory generalization test to activate the DREADD construct. Results revealed a main effect of the DREADD manipulation (F[2, 37=18.9; p<.001). In the hM3Dq group, both GS and ITI-elicited freezing (ITI data not shown) was reduced compared with the control (p<.001) and hM4Di group (p<.001) (Figure 1E). There was also a smaller, but significant, effect of the DREADD manipulation on pre-CS freezing (F[2, 37=4.1; p=.024). hM3Dq mice froze less than hM4Di (p=.027). These data indicate IL excitatory stimulation suppresses the expression of auditory, and to a lesser extent, contextually

459 conditioned generalized freezing. hM4Di mice were not different from controls. There were no

460 sex differences detected throughout.

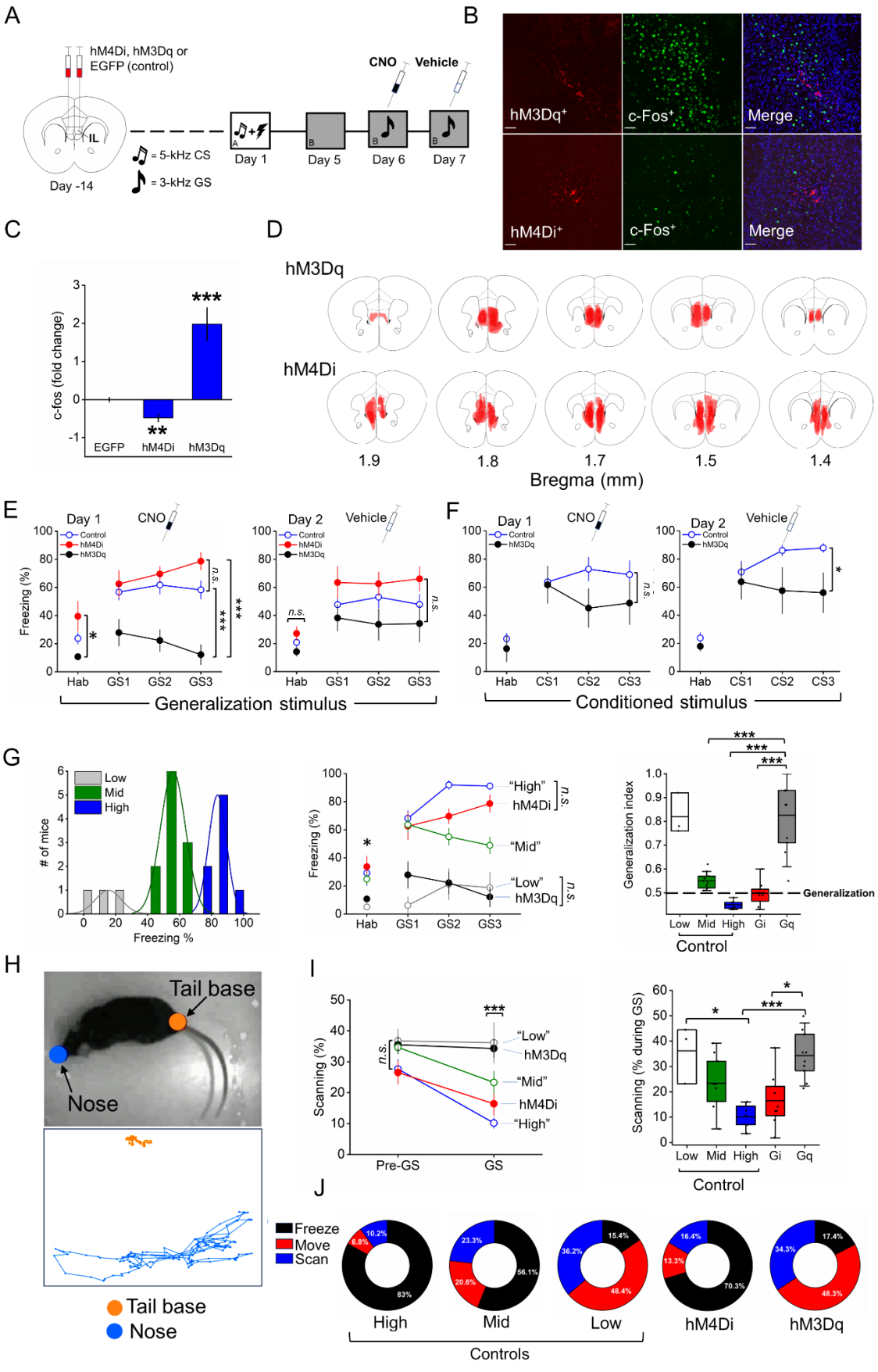

Figure 1. Bidirectional chemogenetic IL manipulation during fear generalization expression. (A) Experimental design. (B) Representative confocal micrographs showing AAV expression (left panel), c-Fos FIH (middle panel), and AAV/c-Fos/DAPI co-expression (20X/0.8 N.A. air). Scale bar = 25 microns. (C) There was a 2-fold increase in c-Fos expression in hM3Dq mice (n=4) and nearly 0.5-fold decrease in c-Fos expression in hM4Di mice (n=6) versus controls (n=6). (D) The extent of AAV expression in the mPFC across five coronal planes is depicted. Relatively darker shaded regions show greater overlap across individuals. Transfection was predominantly located in the IL, with some expression in DP. Mouse brain atlas images modified from (Paxinos & Franklin, 2004). (E) IL stimulation (hM3Dq; n=10) reduced freezing to the context, 3-kHz GS stimulus, and during the intertrial interval (ITI) compared with hM4Di mice (n=8) and fluorophore controls (n=22). There were no differences in freezing across groups on the following day in response to a vehicle control injection. (F) In a separate group of mice, there was no CNO-induced differences between hM3Dq (n=5) and control (n=12) mice in response to CS presentation. The next day, after vehicle injection there was reduced freezing in the hM3Dq group. (G) A k-means clustering algorithm split fluorophore-control mice into low (n=3), middle (n=11), and high (n=8) generalization groups. hM3Di mice exhibited a freezing response like the high generalization control group and hM4Dq mice exhibited a freezing response like the low generalization group. Analysis of the generalization index confirmed these results. (H) DeepLabCut analysis of scanning behavior. (Top panel) markers for pose estimation on the tail base and nose and (bottom panel) representative path analysis depicting low activity in tail base and high activity in nose (scanning). A high proportion of all movement in hM4Dq mice was accounted for by scanning behavior (34%). Mice in the hM4Dq groups showed greater scanning relative to the hM3Di group and “low” generalization control group. Donut plots depict percentage freezing, scanning, and moving during the mean GS presentations. *p<.05 **p<.01, ***p<.001, n.s., non-significant.

In our paradigm, and especially in these initial experiments, presentation of GS produced relatively high levels of generalized freezing (60.5%) and relatively high variance (SD: 23.5). This finding led us to examine individual differences in generalized responses. An unsupervised k-means clustering algorithm was applied to mean GS freezing levels to segregate fluorophore-control mice into high, mid, and low groups (Figure 1F). A reanalysis of the fear conditioning acquisition data showed no differences between low, mid and high groups, indicating the behavioral phenotype is not present during learning. A reanalysis of the DREADDs data showed no difference in freezing between “high generalization” controls and the hM4Di group (p=.79) and no difference in freezing between “low generalization” controls and the hM3Dq group (p=.95). These data suggest IL silencing drives generalization, while IL stimulation promotes less generalized freezing. As a further control, we analyzed data obtained from mice with

unilateral DREADDs expression in IL. Surprisingly, we found no effect of unilateral hM3Dq or DREADDs activation on generalization expression (Figure S2).

IL stimulation and scanning behavior

Next, we asked the question, if hM3Dq mice exhibited reduced freezing to the GS how were they behaving? We speculated that IL stimulation might promote movement classified under "threat detection" (Blanchard et al., 2011), or "pre-encounter threat responses" (Roelofs & Dayan, 2022), such as scanning behavior (Choy et al., 2012). To test this hypothesis, scanning behavior was analyzed using machine learning technology (DeepLabCut2.0) (Mathis et al., 2018; Nath et al., 2019) and custom code. RMANOVA showed a Time x Group interaction ($F[4, 32] = 3.5$; $p = .02$). There were no differences in scanning behavior prior to the presentation of the GS across all groups (Figure 1G). However, upon GS presentation, scanning behavior collapsed in the hM4Di and high generalization control group, but was maintained in the hM3Dq and low generalization group ($F[4, 32] = 9.04$; $p<.001$) (Figure 1G). These data indicate a role for hM3Dq activity in suppressing freezing and maintaining scanning. Interestingly, scanning behavior made-up approximately 50% of all movement across all groups, regardless of DREADDs manipulation. Overall, IL excitatory activity is sufficient to suppress post-encounter defensive responses (freezing) in favor of pre-encounter defensive (scanning) and non-defensive (movement) behaviors in response to an "ambiguous" threat stimulus.

IL stimulation, conditioned freezing, and extinction

Because IL stimulation consistently decreased freezing in response to the GS, an important consideration is the generality of IL function in suppressing conditioned freezing responses. To test this question, we replicated the generalization protocol described above in a separate set of hM3Dq and fluorophore control mice, but rather than presenting the GS, we presented the CS. Results showed no difference in CS-eliciting freezing between hM3Dq and

controls group (Figure 1E). On the following day, the same hM3Dq mice injected with vehicle showed decreased CS-elicited freezing responses (p=.042). These data support previous work showing IL excitation enhances fear memory extinction retention (Quirk et al., 2000).

Brainstem auditory evoked potentials

A fundamental question in the study of stimulus generalization is the consideration that generalized responses may represent a failure in perceptual (sensory) discrimination (Dunzmoor and Paz, 2015), rather than mnemonic processes per se (Zaman et al., 2021). This might confound the present results indicating generalization at the level of forebrain plasticity. To begin to address this question, auditory thresholds using auditory brainstem responses were tested in a subset of ArcCreER^{T2} x eYFP mice. While thresholds cannot determine whether two tones are discriminable from one another, they can address whether tones are likely to be detectable. Evoked potential threshold estimates tend to underestimate behavioral thresholds, so stimuli presented above the AEP threshold should be of sufficient amplitude to evoke behavioral responses. The threshold by frequency response we found is consistent with the patterns in C57BL/6J (B6) mice. Generally, thresholds decreased (i.e. sensitivity improved) as stimulus frequency increased, although the rate of change increased with each subsequent octave. Thresholds at 3 kHz ranged from 57.5 to 67.5 dB SPL, with an average of 62.5 dB SPL (Figure S3). These thresholds are lower than the amplitude of the stimulus used in the generalization experiments, suggesting that individuals should be able to detect this tone. Thresholds do decrease between 4- and 8-kHz, suggesting that the 5-kHz tone may have a greater sensation level than a tone at 3-kHz.

Estimates of auditory filter bandwidth using auditory evoked potentials or psychophysical frequency discrimination limens would further address whether individuals from this strain of mice differ in their ability to discriminate between these tones. C57BL/6J (B6) mice are capable of discriminating frequency changes of 250-Hz or less at 8-kHz, with frequency discrimination

548 decreasing with increasing frequency. Absolute frequency discrimination limens typically
549 decrease with decreasing frequency (Weber's law), suggesting mice should have no difficulty
550 discriminating at 3-kHz tone from a 5-kHz tone. Although sensitivity is lower at 3-kHz than at 5-
551 kHz, our results suggest that tones of both frequencies should be detectable at 70-75 dB in our
552 subjects.

553 **Experiment 2: Cued fear memory generalization and the passage of time.**

554 Here we tested whether cued fear memory generalization increases over time in
555 ArcCreER^{T2} x eYFP transgenic mice, a finding previously shown in the C57BL/6N substrain
556 (Pollack et al., 2018). All mice were fear conditioned with the 5-kHz CS and then, either 7 days
557 (recent) or 30 days (remote) later, were presented with either the CS again or the GS. At the
558 recent time point, there was less freezing in response to the GS (3-kHz) compared to the CS (5-
559 kHz) (F[1,40]=13.4; p<.001), indicating a degree of reduced generalization (Figure 2B).

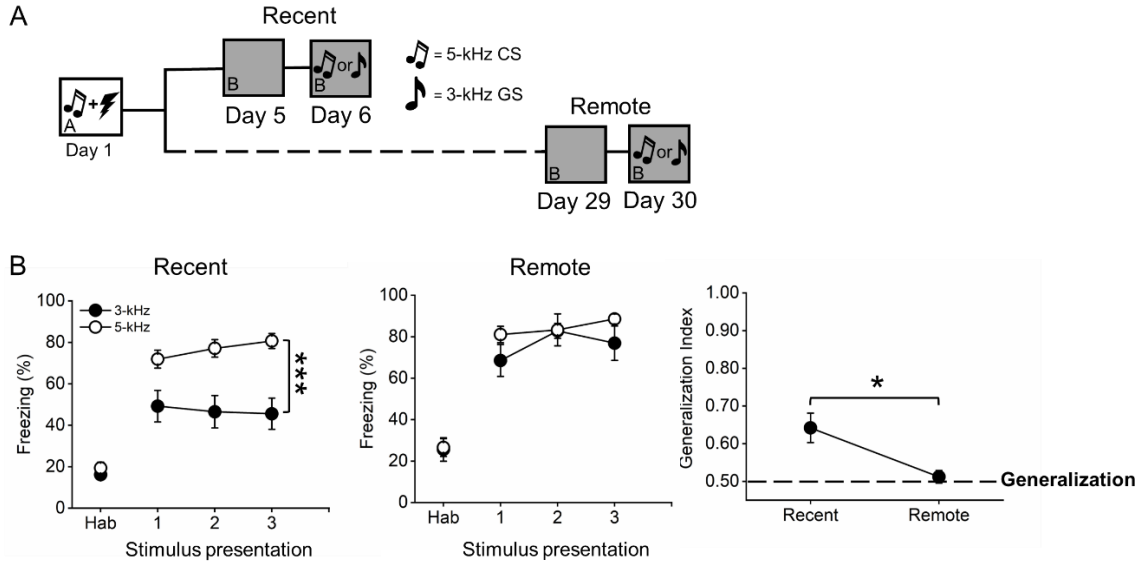

560

561 **Figure 2.** (A) Schematic of the experimental design. (B) At the recent timepoint following
562 learning (7 days), mice in the 3-kHz group exhibited less freezing than the 5-kHz group. At the
563 remote timepoint (30 days), freezing was equivalent between 3-khz and 5-kHz groups. The
564 generalization index reduced, indicating greater generalization compared with the recent
565 timepoint. n=9-21/group. *p<0.05, ***p<0.001.

At the remote time point, there were no differences between the GS and CS groups (p=.58), indicating a greater degree of generalization. Analysis of the generalization index showed a modest, but significant, reduction over time (F[1, 28] = 4.3; p = .045; Figure 2B), indicating enhanced generalization with the passage of time, a finding congruent with previous work (Pollack et al., 2018).

Experiment 3: mPFC neuronal ensemble quantitative measures

In this experiment, a new cohort of mice underwent experiments described in Experiment 2, but 90 min after generalization tests, brain tissue was harvested and processed for Arc immunohistochemistry (IHC). A “no tone” control group was included as a baseline measure in which all procedures were identical to the experimental groups, except that on the test day, mice were not presented with a tone but instead left to explore the context for the same amount of time as the tone stimulus groups (Figure 3A). mPFC neuronal ensembles were tagged using the ArcCreERT2 x eYFP system in which 4-OHT administration induces Cre-mediated recombination and expression of the eYFP reporter in activated neurons (Figure 3B-E). Neurons were counted in PL and IL (Figure 3F).

To assess whether 4-OHT itself might impact fear learning and memory, a separate group of male and female mice were run through the identical behavioral paradigm described above but instead of 4-OHT, they were injected with vehicle (corn oil) control. These mice were compared with mice injected with 4-OHT. Results showed no differences between Group or Sex interactions during either learning or retrieval of the CS (Figure S4). These data indicate 4-OHT does not impact basic fear memory consolidation behavioral performance.

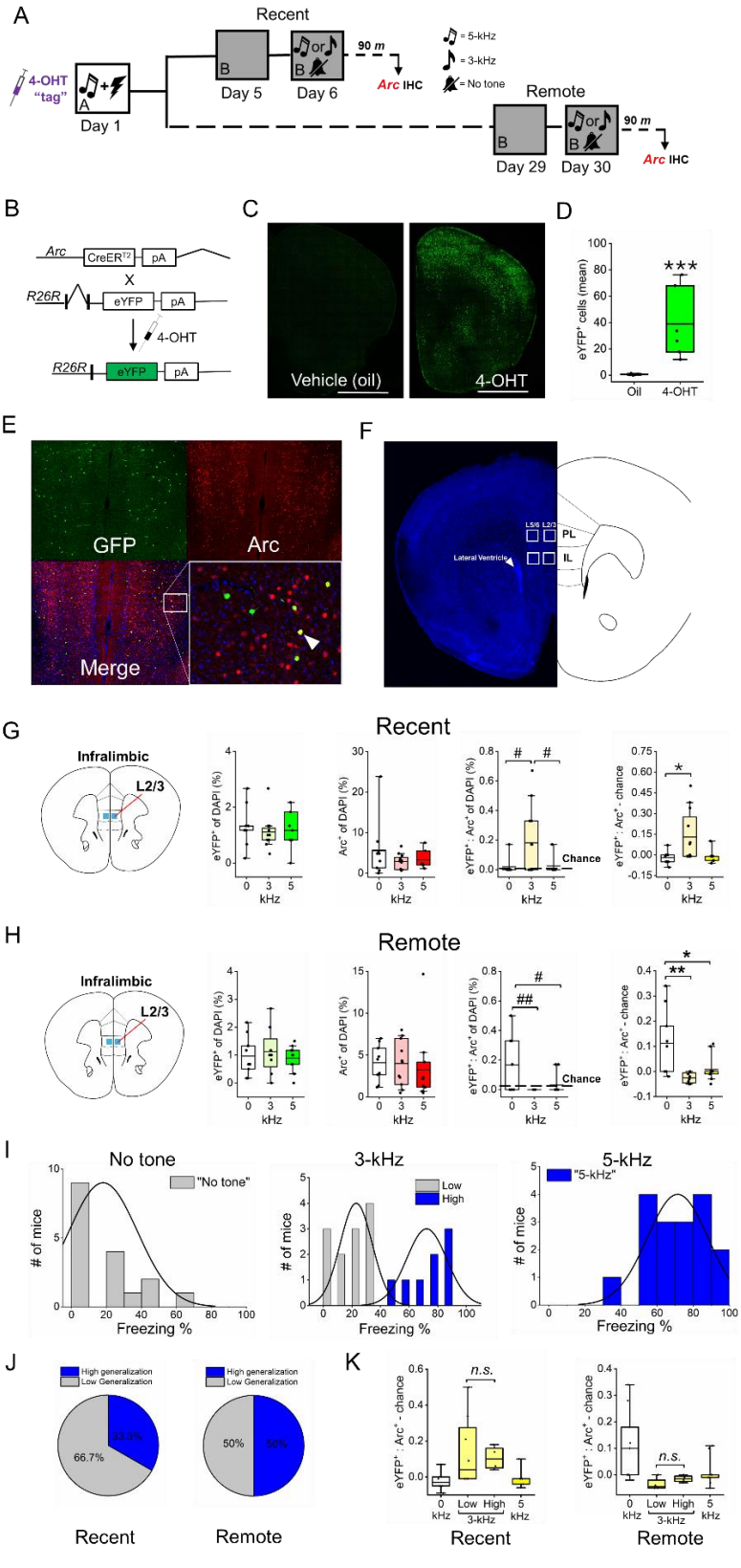

Figure 3. (A) Experimental design. (B) ArcCreERT2 x eYFP system genetic design. (C) Representative photomicrograph depicting the efficacy of 4-OHT to drive eYFP expression after 4-OHT injection versus vehicle control. (D) 4-OHT (n=6) selectively induces eYFP expression (58-fold increase) versus vehicle (oil; n=6) control in ArcCreERT2 mice. (D) Representative photomicrographs depicting GFP and Arc immunofluorescent labeled cells. Arrowhead indicates double-labeled cells. (F) Depiction showing the location of counting frames (250 x 250 microns) in the mPFC. Arrowhead indicates anatomical location of the lateral ventricle. (G) (Recent timepoint) (left panel) Atlas image showing the location of identified neuronal ensemble in IL L2/3. At the recent timepoint, there was no difference in eYFP+ or Arc+ expression across groups. There was a significant, above chance increase in the number of colocalized cells in the 3-kHz group vs. the no tone control and the CS. (H) (Remote timepoint) (Left panel) Atlas image showing the location of identified neuronal ensemble in IL L2/3. At the remote timepoint, there was no difference in eYFP+ or Arc+ expression across groups. There was a significant, above chance, decrease in the number of colocalized cells in the 3-kHz group and increased above chance number of colocalized cells in the no tone group. (I) Frequency diagrams depict the frequency of freezing response within each group. Mice in the 3-kHz group were split into “High” and “Low” generalization groups based on the k-means clustering method. (J) In the 0-kHz no tone control group, there were more “high generalizing” mice at the remote timepoint relative to “low generalization” mice at the recent time point. (K) At either recent or remote timepoints in the high and low generalization groups there was no difference in the number of reactivated cells. n=8-12/group. Hashed lines indicate level of chance calculated as (eYFP +/DAPI+) * (Arc+/DAPI+) * 100. *p< .05 and **p<.01, #p<.05 and ##p<.01 compared to chance.

MANOVA conducted on $eYFP^+$ and Arc^+ cell counts revealed no differences across groups at either timepoint (Figure 3G, H). However, MANOVA conducted on co-activated cells revealed an interaction of Time x kHz *(*V=.49, F[4, 40]=4.99; p=.002). Follow-up Bonferroni-corrected ANOVAs revealed a kHz x Time interaction in L2/3 IL only (F[2,54]=8.0; p=.001). At the recent time point, there was a main effect of kHz (F[2,23]=4.7; p=.02) (Figure 3G). There were a greater number of co-activated neurons at an above chance level in the GS group versus control (p=.04) and no difference between the CS group and controls. Strikingly, a main effect of kHz was also observed at the remote timepoint (F[2,25]=6.5; p=.005) (Figure 3H). We found fewer co-activated neurons at below chance rates in the GS group versus control (p=.004) and no difference between CS and control groups. There were no Time, kHz, or Sex factor differences throughout the PL at either the recent (Figure S5), or remote (Figure S6), timepoint following learning.

Given the individual differences we observed in Experiment 1, we also analyzed individual differences here. Results revealed high variance in GS-elicited freezing, both at the recent

(coefficient of variation (CV) = 66%) and remote (CV = 62.5%) timepoints (as opposed to CV = 23% in the CS group). This led us to postulate that individual differences might help explain the association between ensemble activity in IL and high/low generalization responses. We again used the k-means clustering algorithm to segregate mice into low and high generalization phenotypes within recent and remote timepoints (Figure 3I-J). Surprisingly, results revealed no difference in the number of co-activated cells between high and low generalization phenotypes in GS group at either time point (Figure 3K). This result suggests that identified neuronal ensembles do not scale their reactivation patterns with respect to individual differences in freezing. Rather, their dynamics during a generalization task are tone and time responsive.

Interestingly, the observed increase in the number of IL L2/3 reactivated cells at an above chance rate in the “no tone” control group at the remote timepoint only (Figure 3H), suggests the possibility that a neuronal ensemble associated with the context elements of the chamber (context fear generalization or extinction) was formed. To address this possibility, we analyzed “context B” habituation data to determine if, 1) mice in the remote group showed increased context fear memory generalization over time, as has been shown previously (Wiltgen & Silva, 2007) and, 2) context extinction retention performance. Analysis of the “context B” behavioral data from the day prior to the cued fear memory generalization test showed a Time x Condition interaction (F[3.5, 173.9] = 3.5; p=.005). Mice in the remote group showed greater freezing during the first 3 min of the context test relative to mice in the recent group (F[1, 52] =

644 7.6; p = .008) (Figure 4A).

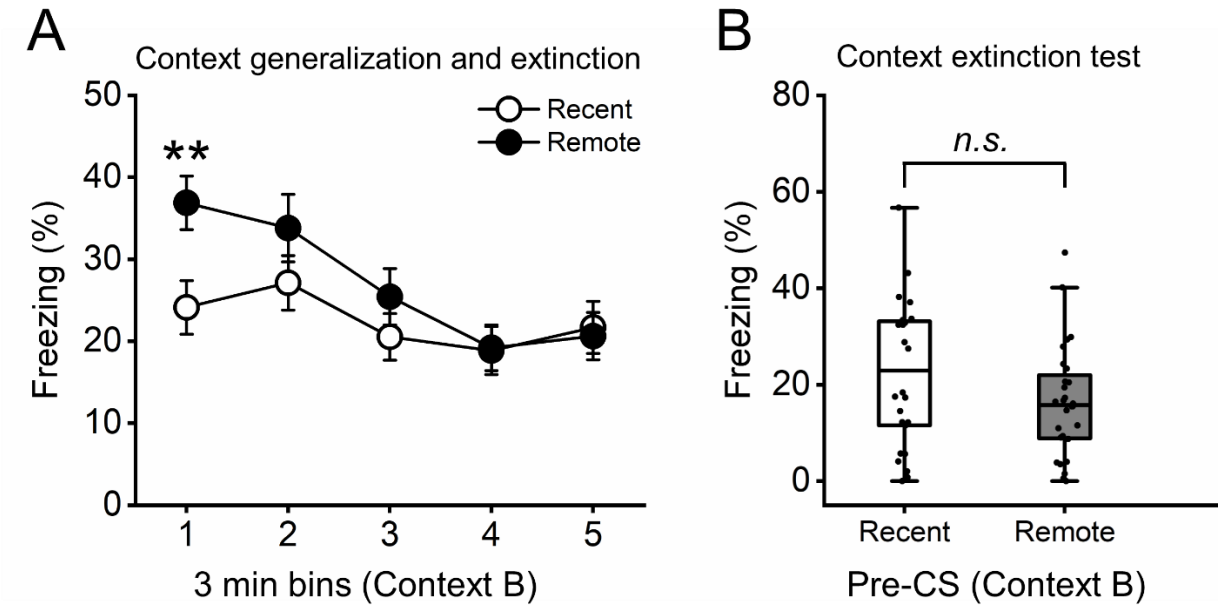

645

646 **Figure 4.** (A) When were placed into novel context B, mice in the Remote group showed more
647 freezing than the Recent group, indicating context generalization increased with the passage of
648 time. There was also significant extinction over the 15 m session. (B) The next day, during the
649 pre-tone period, there was no differences between groups, indicating strong contextual
650 generalization extinction retention **p<.01. n=30-31/group

651 This finding supports previous data showing increased contextual fear memory
652 generalization with the passage of time (Poulos et al., 2016; Wiltgen & Silva, 2007). The
653 difference in the generalized context response declined rapidly over the session and showed no
654 retention the next day (Figure 4B), indicating robust extinction retention of context generalization
655 at the remote time point. This behavioral result was associated with a greater number of
656 reactivated cells during context memory retrieval (pre-GS period), suggesting a neuronal
657 ensemble associated with either greater, 1) context generalization memory or, 2) generalized
658 context fear extinction was formed in IL L2/3 and was expressed during the context test (Figure
659 3H).

660 **Experiment 4: Bidirectional IL chemogenetic neuronal ensemble control during the**
661 **expression of cue fear memory generalization**

In this experiment, a Cre-dependent hM4Di, hM3Dq, or mCherry control was injected into IL to selectively express DIO-hM4Di, DIO-hM3Dq or DIO-mCherry in ArcCreERT2 x eYFP mice (Figure 5A). Subject underwent 4-OHT-dependent tagging during fear conditioning and later retrieval induced neuronal ensemble Arc reactivation was induced using DCZ (Figure 5A).

The efficacy of DCZ to modulate neuronal activity in DIO-DREADD expressing cells, was assayed using IHC against eYFP and Arc. Results revealed no differences in $eYFP^+$ or Arc^+ neuronal expression across groups (Figure 5B-C). When the number of $eYFP^+$:Arc^+ co-localized cells was analyzed, we found a difference across groups (F[2, 14]=15.2; p<.001). There were a greater number of co-activated cells in the DIO-hM3Dq group compared with the control (p<.05) and DIO-hM4Di group (p<.001) (Figure 5C). These data indicate the combination of DCZ and the DIO-DREADD system preferentially drives Arc^+ expression in eYFP-labeled cells. Analysis plotting the spread of viral transfection across brains showed clear AAV transfection in IL and also in DP (Figure 5D). We grouped both bilateral and unilateral transfection into the analysis because there was a high degree of laterality in the expression of eYFP which may have anatomically biased transfection. In addition, there were no statistical differences between bilateral and unilateral were detected between groups. We also grouped controls as there was no difference in freezing over time and allowed for a higher-powered cluster analysis.

By chemogenetically manipulating the activity of a neuronal ensemble established during learning, here we test its contribution to the expression of generalization. Results revealed a main effect of DIO-DREADD manipulation (F[3, 28]=12.0; p<.001). Mice in the DIO-hM3Dq group showed less GS-elicited freezing than mice in the DIO-hM4Di group (p=.002) (Figure 5E). Moreover, DIO-hM3Dq did not differ from low generalizers and DIO-hM4Di did not differ from high generalizers. There was also an effect of DIO-DREADD during the pre-GS period (Hab) (F[3, 28]=3.9; p=.019). Mice in the DIO-hM4Di group froze more than low generalizers (p=.034).

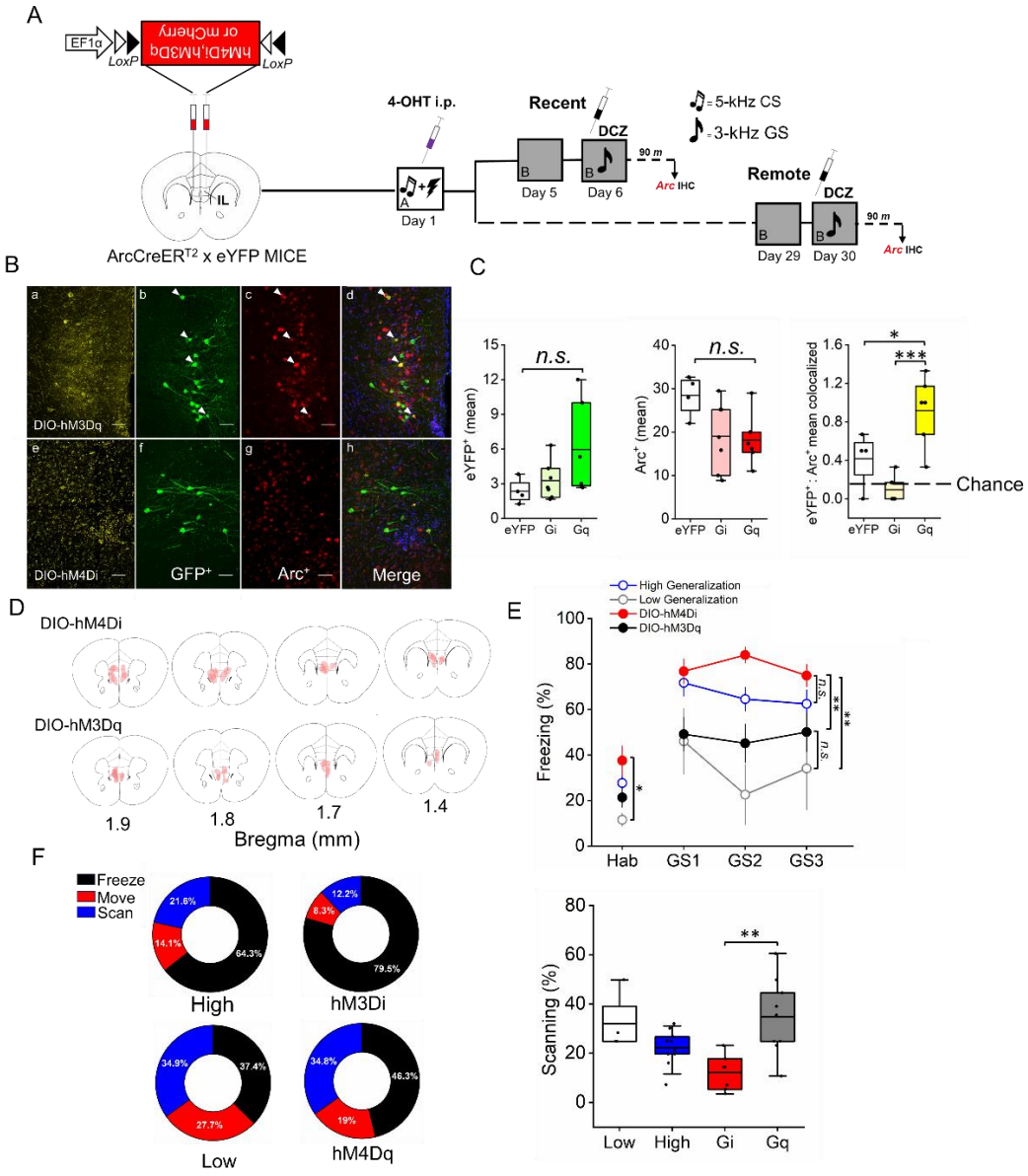

686

687 **Figure 5.** (A) Schematic depicting DIO-DREADD x ArcCreER^{T2} system design and experimental
688 timeline. (B) Representative photomicrographs showing (a) hM3Dq AVV transfection in mPFC,
689 (b) GFP-labeled cells, (c) Arc-labeled cells, (d) image merge (20X, 0.8 N.A., 1.5 zoom).
690 Arrowheads indicate double-labeled GFP$^+$:Arc$^+$ cells. (C) DCZ injection in the DIO-hM3Dq
691 system (n=6) increased the number of co-localized cells relative to DIO-h4Di mice (n=6) and
692 controls (n=4). There was a decrease in DIO-h4Di mice (n=7) versus controls. (D) Heatmapping
693 depicting transfection localized in vmPFC, including IL and DPP. (E) Mice in the DIO-hM3Dq
694 group showed less freezing than DIO-hM4Di mice during presentation of the GS. There was
695 also a difference between mice in the hM4Di group and the low generalization group (left panel).
696 (F) Donut plots depict percentage freezing, scanning, and moving during GS presentation
697 (middle panel). Mice in the DIO-hM3Dq spent more time scanning and moving compared with
698 DIO-hM4Di mice. The control group was collapsed across time according to the mean GS
699 response. n=8-22/group. *p<.05, **p<.01, ***p<.001. Scale bar = 50 μm.

Although not a direct test of contextual fear memory generalization, the observation that mice in the DIO-hM4Di group froze more than the low generalization group supports our previous data supporting a role for IL in contextual fear memory generalization (Figure 5E). As we also saw in Experiment 1, reduced freezing in DIO-hM3Dq mice was associated with a higher degree of scanning behavior relative the DIO-hM4Di group (p<.01) (Figure 5E). Overall, these results indicate IL neuronal ensembles contribute to the expression of cued and contextual defensive memory generalization. However, given DP transfection in a few of our subjects (Figure 5D), interpretation of these results cannot rule out DP functionality in generalization. Throughout the experiments, no sex interactions were detected.

DISCUSSION

Here we leveraged an ArcCreER^{T2} x eYFP transgenic system to genetically tag IL neurons activated during Pavlovian fear conditioning for later visualization and manipulation during the expression of generalization. Shortly after learning, we found more reactivated IL neurons associated with the GS and silencing these neurons promoted generalization (greater conditioned freezing) and a collapse in scanning behavior. Conversely, later after learning, fewer reactivated IL neurons were associated with the GS, and stimulating these neurons promoted less generalized freezing and more scanning. One interpretation of these results is that an IL neuronal ensemble encoding an inhibitory process for attenuating generalized freezing was formed in the IL during initial memory consolidation and expressed in the presence of the GS. This empirical finding confirms a long-standing theory proposing generalization as a learning process (Hull, 1943), and recent work showing that injections of picrotoxin into the IL after learning reduced subsequent freezing during extinction (Bayer et al., 2024). Another important interpretation of these results is that when IL, and IL neuronal ensemble reactivation was suppressed, generalization increased, suggesting mechanisms for generalization expression operate outside IL, perhaps in amygdala (Rajbhandari et al., 2016), anterior cingulate cortex, ventral hippocampus (Cullen et al., 2015), or auditory thalamus (Han et al., 2008).

Another interpretation of our recent timepoint results is that presentation of a similar, but novel, GS promoted IL neuronal ensemble reactivation and memory specificity, presumably because memory for the original CS was intact. Over time, some attribute of the CS (i.e., frequency) may have been forgotten (Bouton et al., 1999), resulting in reactivation failure and the expression of generalization. A key outstanding question is whether the identical IL neuronal ensemble reactivated in response to the GS presented shortly after learning was inactivated at the remote timepoint after learning.

IL functional neuroanatomical heterogeneity

These data support previous findings showing, 1) that the passage of time increases generalization (Pollack et al., 2018; Poulos et al., 2016; Wiltgen & Silva, 2007), 2) a selective role for the IL in processing uncertain threat stimuli (Glover et al., 2020) and, 3) involvement of IL L2/3 plasticity in generalization processes (Pollack et al., 2018; Scarlata et al., 2019). Amongst these findings, the anatomical functional selectivity of IL L2/3 plasticity underlying cued fear memory generalization over time is of particular interest with respect to neuroanatomical heterogeneity within IL layers and between mPFC subregions. There is evidence indicating IL L2/3 neurons are more excitable than PL neurons (Song & Moyer, 2017) and these same neurons preferentially target amygdala but not periaqueductal grey (Ferreira et al., 2015). There is also data indicating IL L2/3 neurons project more heavily to both BLA and the nucleus accumbens as compared to L5 neurons (Bloodgood et al., 2018) and BLA inputs preferentially target L2/3 (McGarry & Carter, 2016). Therefore, unique anatomical connectivity may confer functional selectivity of fear memory generalization-induced plasticity in IL L2/3.

Cued fear memory expression, cued extinction, generalized contextual extinction, and IL functionality.

Cued fear memory expression was spared during IL stimulation. However, on the next day without CNO, cued fear memory expression decreased. We speculate that a brief CS exposure schedule (3 random ITI presentations) may have acted as a “weak” extinction training regimen that, in combination with IL chemogenetic stimulation, promoted stronger extinction retention the next day. This finding supports IL functionality in fear extinction consolidation rather than learning (Bloodgood et al., 2018; Bukalo et al., 2015; Quirk et al., 2000). In addition, these data support a role linking IL functionality in both fear generalization and extinction processes (Bayer & Bertoglio, 2020).

At the remote timepoint only, the “no tone” control group was associated with more L2/3 reactivated cells. We hypothesize this ensemble was associated with the emergence of a new contextual fear extinction memory. The reasoning behind this hypothesis is that all mice were placed into alternate “context B” a day prior to memory reactivation which effectively served as a context generalization test and extinction session. Analysis of these data showed increased context generalization over time, a finding that supports previous work (Wiltgen & Silva, 2007). There was also a reduction in freezing over the test session (extinction) and no difference in freezing on the generalization test day between recent and remote groups, indicating strong contextual fear memory extinction retention. Together, these data suggest a separate IL L2/3 neuronal ensemble was formed and associated with context generalization extinction. Further, fewer co-activated cells in both GS and CS groups implies that the presentation of the tone stimuli may have suppressed reactivation related to contextual extinction. Overall, these data support a role for the IL in context fear extinction (Brockway et al., 2023), context generalization (Bayer & Bertoglio, 2020), and the extinction of generalized contextual fear.

Memory precision and a theoretical basis for dynamic changes in IL ensemble activity over time.

At the remote timepoint following learning, neuronal ensemble activity in response to the GS was reduced. There are several plasticity-related mechanistic possibilities that might account for this phenomenon: 1) IL gradually disengaged its obligatory top-down inhibitory role in the defensive memory circuit over time to support increased generalization, in a systems consolidation-like process (Bergstrom, 2016), 2) IL activity or IL neuronal ensemble reactivation may have been suppressed over time via gradually recruited inhibitory mechanisms (Morrison et al., 2016), or 3) IL neuronal ensemble activity may have weakened over time through a synapse destabilization mechanism, in a process akin to forgetting (Ryan & Frankland, 2022).

With respect to possibilities 2 and 3, one proposal is that neuronal networks employing mechanisms of instability, such as synaptic decay, elimination, or suppression, would promote a greater degree of generalization (Richards & Frankland, 2017). A weakening of synapses (destabilization) may provide a "forgetting" mechanism to promote brain states that reflect the past. That is, in the face of threat ambiguity and over time, it may be advantageous to promote or bias the original CR to enhance the chance of survival in "a better safe than sorry" strategy (Eilam et al., 2011). The exact nature of the suppression of IL L2/3 neuronal ensemble reactivation with respect to generalization processes remains an open question.

Risk assessment, switching defensive states, and IL functionality

In the presence of potential threat, organisms must first detect the threat and then respond, with the most appropriate defensive stance. Predatory Imminence Continuum Theory organizes potential defense responses along a spectrum, from safety (i.e., movement related to foraging), to pre-encounter threat (i.e., vigilant behavior such as scanning), to post-encounter threat (i.e., freezing), to threat contact (i.e., circa-strike defense movement related to fight, flight, or panic) (Fanselow, 1994). Most studies examining defensive behaviors in the context of classical Pavlovian fear conditioning paradigms use freezing behavior as a readout of post-encounter acute "fear" or threat detection in response to the CS.

Here, we hypothesized that mice presented with the GS and exhibiting low levels of freezing might engage alternate defensive responses based on the relative ambiguity of perceived threat. Vigilant scanning behavior was identified as a distinguishable, and highly prominent, defensive behavior that aligns with a pre-encounter threat response to the ambiguous tone (Blanchard et al., 2011). When IL was stimulated, scanning behavior made up a substantial portion (over 34%) of all movement and aligned with scanning behavior identified in control mice segregated into the low generalization group (Figure 1H). Conversely, freezing (generalization) was the predominant response when the IL was inhibited. These data indicate

IL functionality in switching defensive states between post- and pre-encounter; IL inhibition resulted in post-encounter, and IL stimulation promoted pre-encounter, defensive states in response to the GS, potentially via downstream signaling with central nucleus of the amygdala (Moscarello & Penzo, 2022). These findings support other work indicating IL in switching behavioral defensive states to promote movement (Halladay & Blair, 2016) and also theoretical work suggesting a role for IL in promoting behaviors that align with the most rigid reading of the associative relationship amongst cues present (Nett & LaLumiere, 2021). While freezing and scanning are categorized as risk assessment behaviors, they are differentiated by the actual or perceived proximity or ambiguity of the threat.

Ventral medial prefrontal cortex and the dorsal peduncular (DP) prefrontal cortex in fear memory generalization

The vmPFC encompasses IL and DP (Botterill et al., 2024). Throughout chemogenetic experimentation, stereotaxic AVV transfection was preferentially targeted to bias away from dmPFC (caudate and PL) in favor of vmPFC. Precise stereotaxic space alignment and mapping of transfection spread across all mice included in data analysis revealed the majority of DREADDs transfection localized to IL, but also to some extant in DP (ventral to IL) (Figure 1D and 4D). This observation is of interest considering functional neuroanatomical work delineating DP in conditioned defensive processes (Borkar et al., 2024; Botterill et al., 2024; Campos-Cardoso et al., 2024). How DP functions in cued fear memory generalization expression remains unknown.

Clinical relevance

The use of novel “ambiguous” stimuli in an auditory cued Pavlovian defensive conditioning paradigm to study brain functionality underlying generalization processes has preclinical utility for the study of PTSD (Dunsmoor & Paz, 2015) and anxiety disorders (Lissek et

al., 2006). In the field of psychology, a “weak situation” refers to a context in which environmental stimuli are less predictive of threat imminence. The ambiguous nature of the environment tends to produce more individual difference variability and has been proposed as a model for studying anxiety (Lissek et al., 2006). In our paradigm, both the contextual elements and auditory tone frequency were shifted, which might account for wide variation in individual differences. Considering the negative valence domain within the Research Domain Criteria (RDoC) framework, the study of potential, but ambiguous, threat has implications for the study of anxiety that can be differentiated from acute threat (Fanselow & Hoffman, 2024). The vmPFC functions in the expression of generalization in humans (Spalding, 2017) and vmPFC dysfunction has been associated with PTSD and anxiety-related disorders (Alexandra Kredlow et al., 2022). The consensus of data presented here indicates vmPFC functionality, and perhaps vmPFC neuronal ensembles, in “down-shifting” defensive behavioral states. IL is considered a putative analog of Area 25 in humans, which regulates mood and emotion (Alexander et al., 2019). Thus, the methodology and data in this set of experiments may add preclinical value for understanding the role of IL (Area 25) and generalization phenomenon seen in anxiety and trauma-related disorders.

Financial Disclosures: All authors have no conflicts of interest to declare.

Funding information: NIMH R15MH127534-01, NSF 2320195, The Vassar College Undergraduate Research Summer Institute (URSI), and the Ruth M. Berger Foundation, to HCB.

Acknowledgments: Authors thank Dr. Lindsay Halladay for reviewing a previous version of the manuscript. Authors thank Kate Carson for experimental technical expertise, Dave Lewis for microscopy expertise, and the Vassar College Animals Resources team, including Paul Gonzalez, Yi Yaun, Gina Coluccio, and Leah Erickson, for expert care of animal resources.

BIBLIOGRAPHY

Alexander, L., Clarke, H. F., & Roberts, A. C. (2019). A Focus on the Functions of Area 25. *Brain Sciences*, *9*(6). https://doi.org/10.3390/brainsci9060129

Alexandra Kredlow, M., Fenster, R. J., Laurent, E. S., Ressler, K. J., & Phelps, E. A. (2022). Prefrontal cortex, amygdala, and threat processing: Implications for PTSD. *Neuropsychopharmacology*, *47*(1), 247–259. https://doi.org/10.1038/s41386-021-01155-7

Barros, V. N., Mundim, M., Galindo, L. T., Bittencourt, S., Porcionatto, M., & Mello, L. E. (2015). The pattern of c-Fos expression and its refractory period in the brain of rats and monkeys. *Frontiers in Cellular Neuroscience*, *9*(Journal Article), 72.

Bayer, H., & Bertoglio, L. J. (2020). Infralimbic cortex controls fear memory generalization and susceptibility to extinction during consolidation. *Scientific Reports*, *10*(1), 1–13.

Bayer, H., Hassell, J. E., Oleksiak, C. R., Garcia, G. M., Vaughan, H. L., Juliano, V. A. L., & Maren, S. (2024). Pharmacological stimulation of infralimbic cortex after fear conditioning facilitates subsequent fear extinction. *Neuropsychopharmacology*. https://doi.org/10.1038/s41386-024-01961-9

Bergstrom, H. C. (2016). The neurocircuitry of remote cued fear memory. *Neuroscience & Biobehavioral Reviews*, *71*(Journal Article), 409–417.

Bergstrom, H. C. (2020). Assaying Fear Memory Discrimination and Generalization: Methods and Concepts. *Current Protocols in Neuroscience*, *91*(1), e89.

Blanchard, D. C., Griebel, G., Pobbe, R., & Blanchard, R. J. (2011). Risk assessment as an evolved threat detection and analysis process. *Neuroscience & Biobehavioral Reviews*, *35*(4), 991–998.

Bloodgood, D. W., Sugam, J. A., Holmes, A., & Kash, T. L. (2018). Fear extinction requires infralimbic cortex projections to the basolateral amygdala. *Translational Psychiatry*, *8*(1), 60.

Borkar, C. D., Stelly, C. E., Fu, X., Dorofeikova, M., Le, Q.-S. E., Vutukuri, R., Vo, C., Walker, A., Basavanhalli, S., Duong, A., Bean, E., Resendez, A., Parker, J. G., Tasker, J. G., & Fadok, J. P. (2024). Top-down control of flight by a non-canonical cortico-amygdala pathway. *Nature*, *625*(7996), 743–749. https://doi.org/10.1038/s41586-023-06912-w

Botterill, J. J., Khlaifia, A., Appings, R., Wilkin, J., Violi, F., Premachandran, H., Cruz-Sanchez, A., Canella, A. E., Patel, A., Zaidi, S. D., & Arruda-Carvalho, M. (2024). Dorsal peduncular cortex activity modulates affective behavior and fear extinction in mice. *Neuropsychopharmacology*, *49*(6), 993–1006. https://doi.org/10.1038/s41386-024-01795-5

Bouton, M. E., Nelson, J. B., & Rosas, J. M. (1999). Stimulus generalization, context change, and forgetting. *Psychological Bulletin*, *125*(2), 171.

Brockway, E. T., Simon, S., & Drew, M. R. (2023). Ventral hippocampal projections to infralimbic cortex and basolateral amygdala are differentially activated by contextual fear and extinction recall. *Neurobiology of Learning and Memory*, *205*, 107832. https://doi.org/10.1016/j.nlm.2023.107832

940 Bukalo, O., Pinard, C. R., Silverstein, S., Brehm, C., Hartley, N. D., Whittle, N., Colacicco, G.,
941 Busch, E., Patel, S., & Singewald, N. (2015). Prefrontal inputs to the amygdala instruct fear
942 extinction memory formation. *Science Advances*, *1*(6), e1500251.

943 Campbell, E. J., & Marchant, N. J. (2018). The use of chemogenetics in behavioural
944 neuroscience: Receptor variants, targeting approaches, and caveats. *British Journal of*
945 *Pharmacology*, *Journal Article*.

946 Campos-Cardoso, R., Desa, Z. R., Fitzgerald, B. L., Moore, A. G., Duhon, J. L., Landar, V. A.,
947 Clem, R. L., & Cummings, K. A. (2024). The mouse dorsal peduncular cortex encodes fear
948 memory. *Cell Reports*, *43*(4).

949 Cazzulino, A. S., Martinez, R., Tomm, N. K., & Denny, C. A. (2016). Improved specificity of
950 hippocampal memory trace labeling. *Hippocampus*, *26*(6), 752–762.

951 Choy, K. H. C., Yu, J., Hawkes, D., & Mayorov, D. N. (2012). Analysis of vigilant scanning
952 behavior in mice using two-point digital video tracking. *Psychopharmacology*, *221*(4), 649–657.
953 https://doi.org/10.1007/s00213-011-2609-5

954 Cooper, S. E., van Dis, E. A. M., Hagenaars, M. A., Krypotos, A.-M., Nemeroff, C. B., Lissek, S.,
955 Engelhard, I. M., & Dunsmoor, J. E. (2022). A meta-analysis of conditioned fear generalization
956 in anxiety-related disorders. *Neuropsychopharmacology*, *47*(9), 1652–1661.
957 https://doi.org/10.1038/s41386-022-01332-2

958 Corches, A., Hiroto, A., Bailey, T. W., Speigel III, J. H., Pastore, J., Mayford, M., & Korzus, E.
959 (2019). Differential fear conditioning generates prefrontal neural ensembles of safety signals.
960 *Behavioural Brain Research*, *360*(Journal Article), 169–184.

961 Cullen, P. K., Gilman, T. L., Winiecki, P., Riccio, D. C., & Jasnow, A. M. (2015). Activity of the
962 anterior cingulate cortex and ventral hippocampus underlie increases in contextual fear
963 generalization. *Neurobiology of Learning and Memory*, *124*(Journal Article), 19–27.

964 Day, H. L., Suwansawang, S., Halliday, D. M., & Stevenson, C. W. (2020). Sex differences in
965 auditory fear discrimination are associated with altered medial prefrontal cortex function.
966 *Scientific Reports*, *10*(1), 1–10.

967 DeNardo, L., & Luo, L. (2017). Genetic strategies to access activated neurons. *Molecular*
968 *Neuroscience*, *45*, 121–129. https://doi.org/10.1016/j.conb.2017.05.014

969 Denny, C. A., Kheirbek, M. A., Alba, E. L., Tanaka, K. F., Brachman, R. A., Laughman, K. B.,
970 Tomm, N. K., Turi, G. F., Losonczy, A., & Hen, R. (2014). Hippocampal memory traces are
971 differentially modulated by experience, time, and adult neurogenesis. *Neuron*, *83*(1), 189–201.

972 Dunsmoor, J. E., & Paz, R. (2015). Fear generalization and anxiety: Behavioral and neural
973 mechanisms. *Biological Psychiatry*, *78*(5), 336–343.

974 Dymond, S., Dunsmoor, J. E., Vervliet, B., Roche, B., & Hermans, D. (2015). Fear
975 generalization in humans: Systematic review and implications for anxiety disorder research.
976 *Behavior Therapy*, *46*(5), 561–582.

977 Eilam, D., Izhar, R., & Mort, J. (2011). Threat detection: Behavioral practices in animals and
978 humans. *Threat-Detection and Precaution: Neuro-Physiological, Behavioral, Cognitive and*
979 *Psychiatric Aspects*, *35*(4), 999–1006. https://doi.org/10.1016/j.neubiorev.2010.08.002

980 Fanselow, M. S. (1994). Neural organization of the defensive behavior system responsible for
981 fear. *Psychonomic Bulletin & Review*, *1*(4), 429–438. https://doi.org/10.3758/BF03210947

982 Fanselow, M. S., & Hoffman, A. N. (2024). Fear, defense, and emotion: A neuroethological
983 understanding of the negative valence research domain criteria. *American Psychologist*, No
984 Pagination Specified-No Pagination Specified. https://doi.org/10.1037/amp0001354

985 Ferreira, A. N., Yousuf, H., Dalton, S., & Sheets, P. L. (2015). Highly differentiated cellular and
986 circuit properties of infralimbic pyramidal neurons projecting to the periaqueductal gray and
987 amygdala. *Frontiers in Cellular Neuroscience*, *9*(Journal Article), 161.

988 Giustino, T. F., & Maren, S. (2015). The Role of the Medial Prefrontal Cortex in the Conditioning
989 and Extinction of Fear. *Frontiers in Behavioral Neuroscience*, *9*(Journal Article), 298.
990 https://doi.org/10.3389/fnbeh.2015.00298

991 Glover, L. R., McFadden, K. M., Bjorni, M., Smith, S. R., Rovero, N. G., Oreizi-Esfahani, S.,
992 Yoshida, T., Postle, A. F., Nonaka, M., Halladay, L. R., & Holmes, A. (2020). A prefrontal-bed
993 nucleus of the stria terminalis circuit limits fear to uncertain threat. *eLife*, *9*, e60812.
994 https://doi.org/10.7554/eLife.60812

995 Guttman, N., & Kalish, H. I. (1956). Discriminability and stimulus generalization. *Journal of*
996 *Experimental Psychology*, *51*(1), 79.

997 Halladay, L. R., & Blair, H. T. (2016). Prefrontal infralimbic cortex mediates competition between
998 excitation and inhibition of body movements during pavlovian fear conditioning. *Journal of*
999 *Neuroscience Research*, *Journal Article*.

1000 Han, J. H., Yiu, A. P., Cole, C. J., Hsiang, H. L., Neve, R. L., & Josselyn, S. A. (2008).
1001 Increasing CREB in the auditory thalamus enhances memory and generalization of auditory
1002 conditioned fear. *Learning & Memory (Cold Spring Harbor, N.Y.)*, *15*(6), 443–453.
1003 https://doi.org/10.1101/lm.993608

1004 Hull, C. L. (1943). *Principles of behavior: An introduction to behavior theory.*

1005 Ison, J. R., Allen, P. D., & O'Neill, W. E. (2007). Age-related hearing loss in C57BL/6J mice has
1006 both frequency-specific and non-frequency-specific components that produce a hyperacusis-like
1007 exaggeration of the acoustic startle reflex. *Journal of the Association for Research in*
1008 *Otolaryngology*, *8*(4), 539–550.

1009 Jacobs, N. S., Cushman, J. D., & Fanselow, M. S. (2010). The accurate measurement of fear
1010 memory in Pavlovian conditioning: Resolving the baseline issue. *Journal of Neuroscience*
1011 *Methods*, *190*(2), 235–239.

1012 Josselyn, S. A., Köhler, S., & Frankland, P. W. (2015). Finding the engram. *Nature Reviews*
1013 *Neuroscience*, *16*(9), 521–534.

1014 Kreutzmann, J. C., & Fendt, M. (2020). Chronic inhibition of GABA synthesis in the infralimbic
1015 cortex facilitates conditioned safety memory and reduces contextual fear. *Translational*
1016 *Psychiatry*, *10*(1), 1–10.

1017 Kreutzmann, J. C., Jovanovic, T., & Fendt, M. (2020). Infralimbic cortex activity is required for
1018 the expression but not the acquisition of conditioned safety. *Psychopharmacology*, *Journal*
1019 *Article*, 1–12.

1020 Lissek, S., Pine, D. S., & Grillon, C. (2006). The strong situation: A potential impediment to
1021 studying the psychobiology and pharmacology of anxiety disorders. *Biological Psychology*,
1022 *72*(3), 265–270. https://doi.org/10.1016/j.biopsycho.2005.11.004

1023 Mathis, A., Mamidanna, P., Cury, K. M., Abe, T., Murthy, V. N., Mathis, M. W., & Bethge, M.
1024 (2018). DeepLabCut: Markerless pose estimation of user-defined body parts with deep learning.
1025 *Nature Neuroscience*, *21*(9), 1281–1289.

1026 McGarry, L. M., & Carter, A. G. (2016). Inhibitory gating of basolateral amygdala inputs to the
1027 prefrontal cortex. *Journal of Neuroscience*, *36*(36), 9391–9406.

1028 McGowan, J. C., Ladner, L. R., Shubeck, C. X., Tapia, J., LaGamma, C. T., Anqueira-González,
1029 A., DeFrancesco, A., Chen, B. K., Hunsberger, H. C., Sydnor, E. J., Logan, R. W., Yu, T.-S.,
1030 Kernie, S. G., & Denny, C. A. (2024). Traumatic Brain Injury–Induced Fear Generalization in
1031 Mice Involves Hippocampal Memory Trace Dysfunction and Is Alleviated by (R,S)-Ketamine.
1032 *Psychological Traumas and Brain Injury*, *95*(1), 15–26.
1033 https://doi.org/10.1016/j.biopsych.2023.06.030

1034 Morrison, D. J., Rashid, A. J., Yiu, A. P., Yan, C., Frankland, P. W., & Josselyn, S. A. (2016).
1035 Parvalbumin Interneurons Constrain the Size of the Lateral Amygdala Engram. *Neurobiology of*
1036 *Learning and Memory*, *Journal Article*.

1037 Moscarello, J. M., & Penzo, M. A. (2022). The central nucleus of the amygdala and the
1038 construction of defensive modes across the threat-imminence continuum. *Nature Neuroscience*,
1039 *25*(8), 999–1008. https://doi.org/10.1038/s41593-022-01130-5

1040 Nagai, Y., Miyakawa, N., Takuwa, H., Hori, Y., Oyama, K., Ji, B., Takahashi, M., Huang, X.-P.,
1041 Slocum, S. T., & DiBerto, J. F. (2020). Deschloroclozapine, a potent and selective
1042 chemogenetic actuator enables rapid neuronal and behavioral modulations in mice and
1043 monkeys. *Nature Neuroscience*, *23*(9), 1157–1167.

1044 Nath, T., Mathis, A., Chen, A. C., Patel, A., Bethge, M., & Mathis, M. W. (2019). Using
1045 DeepLabCut for 3D markerless pose estimation across species and behaviors. *Nature*
1046 *Protocols*, *14*(7), 2152–2176.

1047 Nett, K. E., & LaLumiere, R. T. (2021). Infralimbic cortex functioning across motivated
1048 behaviors: Can the differences be reconciled? *Neuroscience & Biobehavioral Reviews*, *131*,
1049 704–721. https://doi.org/10.1016/j.neubiorev.2021.10.002

1050 Ng, K., Pollock, M., Escobedo, A., Bachman, B., Miyazaki, N., Bartlett, E. L., & Sangha, S.
1051 (2023). Suppressing fear in the presence of a safety cue requires infralimbic cortical signaling to
1052 central amygdala. *Neuropsychopharmacology*, 1–9.

Orr, M. V., & Lukowiak, K. (2008). Electrophysiological and behavioral evidence demonstrating that predator detection alters adaptive behaviors in the snail Lymnaea. *The Journal of Neuroscience : The Official Journal of the Society for Neuroscience*, *28*(11), 2726–2734. https://doi.org/10.1523/JNEUROSCI.5132-07.2008

Pavlov, I. P. (1927). *Conditional reflexes: An investigation of the physiological activity of the cerebral cortex. Journal Article*.

Paxinos, G., & Franklin, K. B. (2004). *The mouse brain in stereotaxic coordinates*. Elsevier.

Paxinos, G., & Franklin, K. B. (2019). *Paxinos and Franklin's the mouse brain in stereotaxic coordinates*. Academic press.

Pollack, G. A., Bezek, J. L., Lee, S. H., Scarlata, M. J., Weingast, L. T., & Bergstrom, H. C. (2018). Cued fear memory generalization increases over time. *Learning & Memory (Cold Spring Harbor, N.Y.)*, *25*(7), 298–308. https://doi.org/10.1101/lm.047555.118

Poulos, A. M., Mehta, N., Lu, B., Amir, D., Livingston, B., Santarelli, A., Zhuravka, I., & Fanselow, M. S. (2016). Conditioning- and time-dependent increases in context fear and generalization. *Learning & Memory (Cold Spring Harbor, N.Y.)*, *23*(7), 379–385. https://doi.org/10.1101/lm.041400.115

Prager, E. M., Bergstrom, H. C., Grunberg, N. E., & Johnson, L. R. (2011). The importance of reporting housing and husbandry in rat research. *Frontiers in Behavioral Neuroscience*, *5*(Journal Article), 38. https://doi.org/10.3389/fnbeh.2011.00038

Prager, E. M., Chambers, K. E., Plotkin, J. L., McArthur, D. L., Bandrowski, A. E., Bansal, N., Martone, M. E., Bergstrom, H. C., Bespalov, A., & Graf, C. (2018). Improving transparency and scientific rigor in academic publishing. *Journal of Neuroscience Research*, *Journal Article*.

Quirk, G. J., Russo, G. K., Barron, J. L., & Lebron, K. (2000). The role of ventromedial prefrontal cortex in the recovery of extinguished fear. *Journal of Neuroscience*, *20*(16), 6225–6231.

Rajbhandari, A. K., Zhu, R., Adling, C., Fanselow, M. S., & Waschek, J. A. (2016). Graded fear generalization enhances the level of cfos-positive neurons specifically in the basolateral amygdala. *Journal of Neuroscience Research*, *94*(12), 1393–1399. https://doi.org/10.1002/jnr.23947

Reijmers, L. G., Perkins, B. L., Matsuo, N., & Mayford, M. (2007). Localization of a stable neural correlate of associative memory. *Science (New York, N.Y.)*, *317*(5842), 1230–1233.

Richards, B. A., & Frankland, P. W. (2017). The Persistence and Transience of Memory. *Neuron*, *94*(6), 1071–1084.

Roelofs, K., & Dayan, P. (2022). Freezing revisited: Coordinated autonomic and central optimization of threat coping. *Nature Reviews Neuroscience*, *23*(9), 568–580.

Ryan, T. J., & Frankland, P. W. (2022). Forgetting as a form of adaptive engram cell plasticity. *Nature Reviews Neuroscience*, *23*(3), 173–186.

Sangha, S., Diehl, M. M., Bergstrom, H. C., & Drew, M. R. (2020). Know safety, no fear. *Neuroscience & Biobehavioral Reviews*, *108*(Journal Article), 218–230.

1091 Sangha, S., Robinson, P. D., Greba, Q., Davies, D. A., & Howland, J. G. (2014). Alterations in
1092 reward, fear and safety cue discrimination after inactivation of the rat prelimbic and infralimbic
1093 cortices. *Neuropsychopharmacology*, *39*(10), 2405.

1094 Scarlata, M., Lee, S., Lee, D., Kandigian, S., Hiller, A., Dishart, J., Mintz, G., Wang, Z., Coste,
1095 G., & Mousley, A. (2019). Chemogenetic stimulation of the infralimbic cortex reverses alcohol-
1096 induced fear memory overgeneralization. *Scientific Reports*, *9*(1), 6730.

1097 Shepard, R. N. (1987). Toward a universal law of generalization for psychological science.
1098 *Science (New York, N.Y.)*, *237*(4820), 1317–1323.

1099 Song, C., & Moyer, J. R., Jr. (2017). Layer- and Subregion-Specific Differences in the
1100 Neurophysiological Properties of Rat Medial Prefrontal Cortex Pyramidal Neurons. *Journal of*
1101 *Neurophysiology*, *Journal Article*, jn.00146.2017. https://doi.org/10.1152/jn.00146.2017

1102 Sotres-Bayon, F., Cain, C. K., & LeDoux, J. E. (2006). Brain mechanisms of fear extinction:
1103 Historical perspectives on the contribution of prefrontal cortex. *Biological Psychiatry*, *60*(4), 329–
1104 336.

1105 Spalding, K. N. (2017). *The Role of the Medial Prefrontal Cortex in the Generalization of*
1106 *Conditioned Fear. Journal Article*.

1107 Tayler, K. K., Tanaka, K. Z., Reijmers, L. G., & Wiltgen, B. J. (2013). Reactivation of neural
1108 ensembles during the retrieval of recent and remote memory. *Current Biology*, *23*(2), 99–106.

1109 Watson, J. B., & Rayner, R. (1920). Conditioned emotional reactions. *Journal of Experimental*
1110 *Psychology*, *3*(1), 1.

1111 Wiltgen, B. J., & Silva, A. J. (2007). Memory for context becomes less specific with time.
1112 *Learning & Memory (Cold Spring Harbor, N.Y.)*, *14*(4), 313–317.

1113 Zaman, J., Chalkia, A., Zenses, A.-K., Bilgin, A. S., Beckers, T., Vervliet, B., & Boddez, Y.
1114 (2021). Perceptual variability: Implications for learning and generalization. *Psychonomic Bulletin*
1115 *& Review*, *28*(1), 1–19. https://doi.org/10.3758/s13423-020-01780-1

1116